Published in final edited form as:
Am J Physiol Heart Circ Physiol. 2007 December ; 293(6): H3506–H3516.

Cellular and subcellular alternans in the canine left ventricle

Jonathan M. Cordeiro[1], **Jane E. Malone**[1], **José M. Di Diego**[1], **Fabiana S. Scornik**[1], **Gary L. Aistrup**[2], **Charles Antzelevitch**[1], and **J. Andrew Wasserstrom**[2,3,4]

1 *Masonic Medical Research Laboratory, Utica, New York*

2 *Department of Molecular Pharmacology and Biological Chemistry, Northwestern University Feinberg School of Medicine, Chicago, Illinois*

3 *Department of Medicine (Cardiology), Northwestern University Feinberg School of Medicine, Chicago, Illinois*

4 *Feinberg Cardiovascular Research Institute, Northwestern University Feinberg School of Medicine, Chicago, Illinois*

Abstract

Previous studies indicate that action potential duration (APD) alternans is initiated in the endocardial (END) and midmyocardial (MID) regions rather than the epicardium (EPI) in the canine left ventricle (LV). This study examines regional differences in the rate dependence of Ca^{2+} transient characteristics under conditions that give rise to APD and associated T wave alternans. The role of the sarcoplasmic reticulum (SR) was further evaluated by studying Ca^{2+} transient characteristics in myocytes isolated from neonates, where an organized SR is poorly developed. All studies were performed in cells and tissues isolated from the canine LV. Isolated canine ENDO, MID, and EPI LV myocytes were either field stimulated or voltage clamped, and Ca^{2+} transients were measured by confocal microscopy. In LV wedge preparations, increasing the basic cycle length (BCL) from 800 to 250 ms caused alternans to appear mainly in the ENDO and MID region; alternans were not observed in EPI under these conditions. Ca^{2+} transient alternans developed in response to rapid pacing, appearing in EPI cells at shorter BCL compared with MID and ENDO cells (BCL = 428 ± 17 vs. 517 ± 29 and 514 ± 21, respectively, $P < 0.05$). Further increases in pacing rate resulted in the appearance of subcellular alternans of Ca^{2+} transient amplitude, which also appeared in EPI at shorter BCL than in ENDO and MID cells. Ca^{2+} transient alternans was not observed in neonate myocytes. We conclude that *1*) there are distinct regional differences in the vulnerability to rate-dependent Ca^{2+} alternans in dog LV that may be related to regional differences in SR function and Ca^{2+} cycling; *2*) the development of subcellular Ca^{2+} alternans suggests the presence of intracellular heterogeneities in Ca^{2+} cycling; and *3*) the failure of neonatal cells to develop Ca^{2+} alternans provides further support that SR Ca^{2+} cycling is a major component in the development of these phenomena.

Keywords

alternans; calcium ion transients; heterogeneity

Repolarization or T wave alternans (TWA) is an electrocardiographic (ECG) phenomenon characterized by a beat-to-beat alternation of the amplitude, morphology, and/or polarity of the T wave. Electrical remodeling can occur under a variety of pathophysiological conditions such as acquired and congenital long QT syndromes (33), heart failure (21), and cardiac ischemia (23), producing the conditions for the initiation of arrhythmias (arrhythmogenic

Address for reprint requests and other correspondence: J. M. Cordeiro, Masonic Medical Research Laboratory, 2150 Bleecker St., Utica, NY 13501-1787 (e-mail: jcordeiro@mmrl.edu).

substrate). Despite the link between the appearance of alternans and the development of arrhythmias, the mechanism underlying the development of alternans remains unresolved. Previous studies indicate there are large differences in the magnitude of L-type Ca^{2+} current (I_{Ca}) and the rapid form of the delayed-rectifier K3 current during the long and the short action potentials (APs), suggesting an ionic component to the development of alternans (12,15,18). In contrast, other studies have shown that disruptions in intracellular Ca^{2+} cycling contribute to alternans (8,29). These observations suggest that a major component of alternans is the result of alternation of intracellular Ca^{2+} concentration ($[Ca^{2+}]_i$), which results in secondary changes in the AP in ventricular myocardium (for review, see Ref. 34).

The Ca^{2+} transient that controls cell shortening during excitation-contraction (EC) coupling is a dynamic process that is controlled by Ca^{2+} influx and release as well as Ca^{2+} reuptake and extrusion. A number of studies have highlighted the regional differences in mechanical shortening and $[Ca^{2+}]_i$ cycling across the wall of the left ventricle (LV; see Refs. 6,16,24, and 38). A prominent transient outward K^+ current (I_{to})-mediated phase 1 often present in epicardial (EPI) and midmyocardial (MID) cells contributes to the manifestation of a larger peak I_{Ca} (3, 30,31) and a rapid rise of the calcium transient and mechanical contraction. Endocardial (ENDO) cells exhibit slower contraction and relaxation kinetics than EPI because of intrinsic differences in the contractile proteins between the EPI and ENDO layer as well as slower kinetics of the Ca^{2+} transient (6,24,36). These intrinsic transmural distinctions are thought to synchronize and improve contractile efficiency of the ventricular myocardium under normal conditions. Under pathophysiological conditions, especially during increased heart rate, these heterogeneities may contribute to Ca^{2+} alternans and TWA, reflecting an arrhythmogenic substrate.

In contrast to the adult ventricular myocardium, which exhibits marked heterogeneity (4,11, 25), the AP waveform recorded from the neonatal ventricle appears uniform. In addition, there are a number of structural differences in the neonate ventricle. For example, most newborn ventricular myocytes lack a t-tubular system at birth, but the t-tubular system develops with age (13,32). In addition, sarcoplasmic reticulum (SR) Ca^{2+} release channels (or ryanodine receptors, RyR2) appear to be poorly organized or developed in the neonate ventricle (13, for review, see Ref. 35). These studies demonstrate that the mechanisms underlying EC coupling are different between neonatal and adult ventricles.

Previous studies have shown that action potential duration (APD) alternans, which underlies TWA, is initiated in the ENDO and MID regions vs. EPI in the canine ventricle under long QT conditions (33). The present study examines regional differences in the rate dependence of Ca^{2+} transient characteristics under rapid-pacing conditions that give rise to APD and associated TWA. The role of the SR in the development of alternans is further evaluated by studying Ca^{2+} transient characteristics in myocytes isolated from neonates, where an organized SR is poorly developed. Preliminary results have been presented in abstract form (28).

METHODS

Ventricular wedge preparations

We used arterially perfused canine LV wedge preparations to examine the contribution of beat-to-beat alternation of AP morphology in EPI, MID, and ENDO to ST-T wave and mechanical alternans (9,10). The preparations were perfused oxygenated (95% O_2-5% CO_2) Tyrode solution maintained at 37 ± 0.5°C. The composition of the Tyrode solution was (in mmol/l): 129 NaCl, 4 KCl, 0.9 NaH_2PO_4, 20 $NaHCO_3$, 1.8 $CaCl_2$, 0.5 $MgSO_4$, and 5.5 D-glucose 5.5; pH = 7.4.

Transmembrane APs were simultaneously recorded from EPI, MID, and ENDO using floating microelectrodes (2.7 mol/l KCl, 10–30 MΩ direct current resistance) referenced to ground and connected to a high-input impedance amplification system (World Precision Instruments, New Haven, CT). A transmural pseudo-ECG was recorded using two K^+-Agar electrodes (1.1 mm ID) placed ~1 cm from the EPI (+) and endocardial (−) surfaces of the preparation and along the same axis as the transmembrane recordings. In addition, isometric contractile force was simultaneously recorded; one end of the preparation was fixed to the bottom of the chamber, and the other was attached to a force-displacement transducer (Grass Instruments, Astro-Med, West Warwick, RI) by means of a 4-arm hook. LV wedges were allowed to equilibrate in the chamber for ~2 h while being paced at a basic cycle length (BCL) of 800 ms using silver bipolar electrodes in contact with the endocardial surface.

Ventricular wedge preparations were initially stimulated at BCL = 800 ms using a Pulsar 6i (FHC, Bowdoin, ME) after which the BCL was reduced to 250 ms for 15–30 s. All signals were displayed on Tektronix oscilloscopes, amplified [model 1903-4 programmable amplifiers; Cambridge Electronic Designs (CED)], digitized (model 1401 AD/DA system; CED), analyzed (Spike 2 acquisition and analysis module; CED), and stored on magnetic media (Personal Computer).

Isolation of adult myocytes

Myocytes from EPI, ENDO, and MID regions were prepared from canine hearts using techniques previously described (6,27). Briefly, adult mongrel dogs were anesthetized with pentobarbital sodium (35 mg/kg iv), and their hearts were removed rapidly and placed in nominally Ca^{2+}-free Tyrode solution. A wedge consisting of the LV free wall supplied by a descending branch of the circumflex artery was excised, cannulated, and perfused with nominally Ca^{2+}-free Tyrode solution containing 0.1% BSA for a period of ~5 min. The wedge preparations were then subjected to enzyme digestion with the nominally Ca^{2+}-free solution supplemented with 0.5 mg/ml collagenase (type II; Worthington) and 1 mg/ml BSA for 8–12 min. After perfusion, thin slices of tissue from the EPI (<2 mm from the EPI surface), MID (~5–7 mm from the EPI surface), and ENDO (<2 mm from the ENDO surface) were shaved from the wedge using a dermatome. The tissue slices were then placed in separate beakers, minced, incubated in fresh buffer containing 0.5 mg/ml collagenase and 1 mg/ml BSA, and agitated. The supernatant was filtered and centrifuged at 200 rpm for 2 min, and the pellet containing the myocytes was stored in 0.5 mM Ca^{2+} HEPES buffer at room temperature.

Isolation of neonate cells

Myocytes were prepared from 2- to 3-wk-old canine hearts. Male and female mongrel dogs were anesthetized with pentobarbital sodium (35 mg/kg iv), and their hearts were removed rapidly and placed in nominally Ca^{2+}-free Tyrode solution. The heart was then cannulated through the aorta and perfused with nominally Ca^{2+}-free Tyrode solution containing 0.1% BSA for a period of ~5 min. The heart was subjected to enzymatic digestion with the nominally Ca^{2+}-free solution supplemented with 0.5 mg/ml collagenase (type II; Worthington), 1 mg/ml BSA, and 30 mM 2,3-butanedione monoxime (BDM) for 7–9 min. After perfusion, the LV was removed, minced, and incubated in fresh buffer containing 0.5 mg/ml collagenase, 1 mg/ml BSA, and 30 mM BDM and agitated. The supernatant was filtered and centrifuged at 200 rpm for 2 min, and the pellet containing the myocytes was stored in Kraftbruhe (KB) solution at room temperature. This investigation conforms to the *Guide for the Care and Use of Laboratory Animals* published by the National Institutes of Health (NIH publication No 85-23, Revised 1996) and was approved by the Animal Care and Use Committee of the Masonic Medical Research Laboratory.

Fluorescence imaging

Fluo 4-AM was used. About 1.5 ml of cell suspension containing either EPI, ENDO, MID, or neonate cells were added to the fluo 4-AM [dissolved in 20% F-127 pluronic in dimethyl sulfoxide (DMSO), final concentration ~15 μM] for 20 min at room temperature as previously described (7).

All confocal experiments were performed with an Olympus Fluoview laser-scanning confocal microscope. Fluo 4-loaded myocytes were placed in a perfusion chamber and excited at 488 nm using an argon laser, and fluorescence emission was detected via a 520-nm band-pass filter and photomultiplier tube. Myocytes were repetitively field stimulated (3-ms duration square wave pulse delivered via a pair of platinum wires) at various BCLs (Pulsar 6i; FHC). Confocal images were acquired with the Fluoview acquisition software program and recorded on a personal computer for later analysis. Images acquired with Fluoview acquisition software were analyzed with ImageJ or Transform (Noesys, Boulder, CO). All confocal experiments were performed at 36°C.

Staining with di-8-ANEPPS

Myocytes were stained with the membrane-selective dye di-8-ANEPPS. Cells were exposed to 5 μM of dye (dissolved in DMSO + 20% F127 pluronic) for 5 min. After washout, cells were excited at 488 nm, and the emitted signal was recorded at 520 nm.

Immunofluorescence labeling of RyRs

RyR2 were localized in ventricular cells using previously described techniques (7). The primary (1°) antibody was diluted in 10% goat serum at a concentration of 0.5–1.0 μg/ml. The secondary (2°) antibody was then added to the fixed myocytes for 4 h. As a control, the 2° antibody alone was added to fixed myocytes. The 2° antibody was goat anti-mouse Alexa dissolved in PBS. RyR2 receptor antibody conjugated to Alexa was visualized by confocal microscopy using 488 nm excitation with emission detected at 520 nm.

Myocyte solutions

All solutions were made with Milli-Q grade water. The modified storage (KB) solution had the following composition (in mmol/l): 100 potassium glutamate, 10 potassium aspartate, 25 KCl, 10 KH_2PO_4, 2 $MgSO_4$, 20 taurine, 5 creatine, 0.5 EGTA, 20 glucose, 5 HEPES, and 0.2% BSA. Myocytes were superfused with an external HEPES buffer of the following composition (in mmol/l): 140 NaCl, 4 KCl, 1.0 $MgCl_2$, 1.8 $CaCl_2$, 10 HEPES, and 10 glucose, pH = 7.4 with NaOH.

Electrophysiological recordings

Simultaneous voltage-clamp and confocal recordings of fluo 4-loaded ventricular cells were made. Pipettes were pulled using a gravity puller (model PP-830; Narashige). The internal pipette solution had the following composition (in mmol/l): 113 KCl, 5.5 glucose, 5 K_2ATP, 1.0 $MgCl_2$, 10 HEPES, and 10 NaCl, pH = 7.2 with KOH. Pipette resistance ranged from 1 to 4 MΩ when filled with internal solution. Myocytes were superfused with the external HEPES buffer (described above), ionic currents were recorded with an Axoclamp 1D amplifier (Axon Instruments), and series resistance errors were compensated 65–70%. Membrane currents were recorded and analyzed using pClamp 9.0 software (Axon Instruments).

Drugs

Fluo 4-AM, F-127 pluronic, and di-8-ANEPPS were purchased from Molecular Probes (Eugene, OR). Anti-RyR2 receptor antibody was purchased from Affinity Bioreagents

(Golden, CO). Cytochalasin D and latrunculin B were purchased from Sigma-Aldrich (St. Louis, MO).

Statistics

Results from pooled data are presented as mean ±SE. Statistical analysis was performed using an ANOVA test followed by a Student-Newman-Keul's test or a Student's *t*-test, as appropriate, using SigmaStat software. A $P < 0.05$ was considered statistically significant.

RESULTS

Regional differences in APD alternans in the cardiac ventricular wedge

As an initial basis of comparison, APs and tension were measured simultaneously in EPI, ENDO, and MID layers from the canine LV wedge preparation. Figure 1 shows tension (*top*), AP recordings (*middle*), and an ECG (*bottom*) from a wedge preparation. At a BCL of 800 ms, APs from EPI and MID layers exhibited a prominent spike and dome configuration. The corresponding tension showed a uniform contraction-relaxation cycle. To induce alternans, the pacing rate was changed abruptly from a BCL of 800 to 250 ms. The development of mechanical alternans can be observed in the tension recording, and the ECG shows the appearance of ST-T wave alternans. However, only the MID and ENDO layers exhibited electrical alternans. In seven LV wedge preparations exposed to rapid pacing, APD alternans tended to occur in the ENDO (change in APD at 90% repolarization = 5.7 ± 4.7 ms) and MID (6.8 ± 2.2 ms) layers and was never observed in the EPI (1.0 ± 0.2 ms) layer under these pacing conditions. These data suggest that ENDO and MID layers are more sensitive to the development of pacing-induced APD alternans than the EPI region. As a consequence, transmural heterogeneities in APD and repolarization time are exaggerated on a beat-to-beat basis, thus increasing the likelihood that reentrant arrhythmias might develop.

Characteristics of Ca^{2+} transients across ventricular myocardium

Evidence suggests that a major component of alternans is due to a disruption in the cycling of $[Ca^{2+}]_i$ (34). We investigated the cellular basis for the increased sensitivity of the MID and ENDO regions to develop alternans under rapid pacing conditions. The propensity for MID and ENDO regions to develop alternans may simply be due to longer APDs in these transmural layers (1,27). The longer APDs would result in a longer Ca^{2+} transient, leading to greater susceptibility to disruption of normal Ca^{2+} cycling at rapid rates.

Previous studies have demonstrated that AP waveform and duration can affect the Ca^{2+} transient (6,20,30). To eliminate the influence of the AP waveform and duration, we measured the Ca^{2+} transient under voltage-clamp conditions. Figure 2 shows representative ion channel currents and corresponding Ca^{2+} transients recorded from fluo 4-loaded EPI, MID, and ENDO cells during a 300-ms square pulse. Before application of the test pulse, five square prepulses were applied at a BCL = 500 ms to maintain a uniform SR Ca^{2+} content (26). A large inward Na^+ current was recorded in all three cell types in response to a depolarization to +20 mV (Na^+ current truncated for clarity). A prominent I_{to} was also observed in both EPI and MID cells (Fig. 2, *top*). The corresponding confocal xt line scan shows a rapid rise in Ca^{2+} throughout the cell upon depolarization (Fig. 2, *bottom*). There were no significant differences in Ca^{2+} transient amplitude (F/F_o) when cells from all three regions were activated by a standard square clamp step (EPI = 2.30 ± 0.08, $n = 7$; MID = 2.29 ± 0.10, $n = 7$; ENDO = 2.34 ± 0.16, $n = 6$). However, upon repolarization, the decay of the Ca^{2+} transient was significantly slower in ENDO cells (664 ± 49.4 ms, $n = 6$) compared with EPI (369 ± 29.1 ms, $n = 6$) and MID (417 ± 44.0 ms, $n = 7$) cells. These results show that differences in the decay of the Ca^{2+} transient persist even when the differences in AP waveform and duration are eliminated.

To compare how Ca^{2+} transients are affected by native AP activation, we next compared Ca^{2+} transients evoked by field stimulation in the three different ventricular cell types. Line scan images were recorded from EPI, MID, and ENDO cells stimulated at a BCL of 1,000 ms (Fig. 3). The line scan images in the three ventricular cell types showed a synchronous increase in fluorescence across the cell. Analysis of F/F_o in the three cell layers revealed that ENDO cells displayed a significantly larger F/F_o (2.68 ± 0.16, n = 16) compared with EPI (2.45 ± 0.14, n = 19) and MID (2.46 ± 0.08, n = 24). More importantly, we found that the duration of the transient is longer in ENDO (610 ± 11.5 ms, n = 15) compared with EPI (475 ± 24.8 ms, n = 12) and MID (569 ± 19.3 ms, n = 12) when activated by the AP at a BCL = 1,000 ms, confirming previous results (5). These results suggest that differences in AP morphology and intrinsic differences in E-C coupling contribute to the regional differences in Ca^{2+} transient characteristics.

Development of Ca^{2+} alternans in different myocardial regions

In our ventricular wedge experiments, rapid pacing led to the development of electrical alternans in cells from the ENDO and MID layers. In addition, ENDO cells displayed a transient decayed larger F/F_o and a slower decay of the Ca^{2+} compared with EPI and MID cells. We next evaluated whether there were differences in the development of Ca^{2+} alternans at the cellular level. In the next series of experiments, fluo 4-loaded ventricular cells were field stimulated at progressively faster rates until Ca^{2+} alternans appeared. In these experiments, the laser was kept at the lowest setting (6%), and the recording time was 3 s to limit damage to the cell. Figure 4 shows representative xt line scans of Ca^{2+} transients recorded from the three ventricular cell types at a cycle length of 800 ms (Fig. 4*A*). The corresponding time course of F/F_o is shown at the bottom of each line scan. Because cells from the three layers were paced at faster rates, alternans in calcium transient amplitude appeared in ENDO and MID first (Fig. 4*B*). Analysis of the three ventricular cell types indicated that the BCL at which alternans first appeared (threshold defined as >15% alternation in beat-to-beat amplitude at steady state) was significantly faster in EPI cells (428 ± 17 ms, n = 5) compared with MID (507 ± 29 ms, n = 5) and ENDO (514 ± 21 ms, n = 7). These data demonstrate that Ca^{2+} alternans develops at the whole cell level in each of the three cell types but that MID and ENDO cells develop alternans at slower pacing rates.

Subcellular alternans in different myocardial regions

In addition to Ca^{2+} alternans that develops uniformly throughout the entire myocyte, we periodically observed subcellular Ca^{2+} alternans manifest as heterogeneities in the amplitude of the Ca^{2+} transients recorded along the length of a single myocyte (2, 8; see Fig. 4*C*). We examined this form of intracellular heterogeneity in Ca^{2+} signaling in the three cell types. Figure 5*A* shows a representative xt line scan recording from a cell exhibiting subcellular Ca^{2+} alternans. In this example, half of the length of the cell displayed alternations in Ca^{2+} levels out of phase with the other half of the cell. The time course of F/F_o shows no alternation in intracellular Ca^{2+} when the fluorescence intensity is integrated across the entire width of the cell (Fig. 5*B*). However, when the change in fluorescence is integrated across half the cell, subcellular alternation is obvious. The profile plot (measured at the arrows in Fig. 5*A*) shows that this alternans was out of phase with the alternans occurring in the other half of the cell (Fig. 5*C*). A three-dimensional reconstruction provides an impression of the distribution of Ca^{2+} during subcellular alternans (Fig. 5*D*). Subcellular alternans was observed in four other ENDO, three MID, and three EPI cells. The BCL where subcellular alternans were observed was faster than the cycle length where cellular alternans were observed (EPI = 405 ± 16 ms; MID = 479 ± 23 ms, and ENDO = 493 ± 17 ms).

To rule out the possibility that subcellular alternans may be due to the cell contracting vigorously and moving out of the confocal plane, we repeated the rapid pacing protocol in the

presence of the contractile inhibitors latrunculin B and cytochalasin D (50 μM each). These contractile inhibitors did not produce a significant change in the duration of the Ca^{2+} transient (EPI = 492.1 ± 35.0 ms, n = 7; MID = 591.4 ± 29.3 ms, n = 7; ENDO = 642.8 ± 16.0 ms, n = 7). In addition, the F/F_o was unchanged (EPI = 2.70 ± 0.24, n = 7; MID = 2.68 ± 0.33, n = 7; ENDO = 2.96 ± 0.36, n = 7), and subcellular alternans developed as it did in their absence (Fig. 5*E*), indicating that subcellular alternans is not a motion artifact. Subcellular alternans was observed in a total of five ventricular cells exposed to the paralytics.

Absence of alternans in the absence of t-tubules

Previous studies have suggested that alternans is due largely to defects in the cycling of intracellular Ca^{2+}, since block of SR function with ryanodine abolishes the development of alternans (33). These observations suggest that alternans should be difficult to induce in cardiac cells in which the SR is poorly developed or organized, as in neonate ventricular myocytes (13).

Using cardiac myocytes isolated from the hearts of both adult and neonatal dogs, we first assessed the presence of a t-tubular system by staining with di-8-ANEPPS. Figure 6*A* showed an absence of t-tubules in myocytes isolated from both 2-wk and 1-mo hearts, suggesting that EC coupling occurs without involvement of these structures, as is normally the case in Purkinje (5) and atrial (17) cells. In addition, we performed immunocytochemistry with antibodies specific for the cardiac isoform of RyR2. Cells were labeled with 1° antibodies raised against RyR2 and visualized with 2° antibody conjugated to Alexa (Fig. 6*B*). Adult ventricular cells showed prominent banding at the level of the t-tubules, suggesting that RyRs were located at sites adjacent to the t-tubules. Interestingly, ventricular cells isolated from 1-mo-old dogs also exhibited RyR bands in the interior of the cell (Fig. 6*B*), but staining patterns indicate that t-tubules were in a formative stage of development (Fig. 6*A*). Cells from 2-wk-old dogs did not show banding, suggesting that RyR2 is not as well organized as in adult ventricular cells. In the absence of 1° antibodies, application of the 2° antibody did not produce any intense regions of labeling (data not shown). Given that the 1° antibody is highly specific for RyR2 (19), we conclude that the RyR2 necessary for Ca^{2+}-induced Ca^{2+} release becomes better organized and represents the adult phenotype at around 1 mo of age.

We repeated the rapid pacing protocol in neonate ventricular myocytes isolated from 2-wk-old animals. Because 2-wk cells lack T tubules, we expected a fluorescence profile similar to that seen in atrial (17) and Purkinje (7) cells. Figure 7 shows an xt line scan image recorded from a 2-wk and 1-mo ventricular cell paced at a cycle length of 1 Hz. In contrast to the adult ventricular cells (Fig. 2), the fluorescence trace showed a “U”-shaped profile with the fluorescence increase at the edge preceding that in the center. Alternans could not be induced at any cycle lengths tested in cells from 2-wk-old animals (0/11 cells). In addition, alternans was absent in 15/17 cells from 1-mo-old animals. The remaining two cells from 1-mo-old animals did develop whole cell alternans, consistent with the finding that the t-system is at various early stages of development at 1 mo.

These observations could be interpreted to suggest that the absence of a t-tubular system may account for the absence of Ca^{2+} alternans. However, these observations, combined with the evidence that ryanodine abolishes alternans, suggest that it is the lack of a functional SR that is responsible for the absence of Ca^{2+} alternans.

DISCUSSION

APD and Ca^{2+} transient alternans across the LV myocardium

Our results demonstrate at the level of the isolated ventricular wedge preparation, ENDO and MID cells show a greater propensity to develop APD alternans at rapid rates of stimulation. The lack of APD alternans of the EPI cells results in beat-to-beat alternation of the transmural voltage gradient giving rise to ST-T wave alternans in the ECG. The appearance of TWA is thought to reflect the presence of an arrhythmogenic substrate (for review, see Ref. 34).

Although there is growing evidence that beat-to-beat differences in Ca^{2+} cycling underlie frequency-dependent APD and TWA, the subcellular mechanisms responsible for Ca^{2+} alternans are not clearly defined. Wan et al. (36) demonstrated that myocytes isolated from guinea pig LV ENDO develop Ca^{2+} alternans at longer BCL than EPI cells and that this difference is not related to any difference in APD. There is also growing evidence that there are differences in expression of Ca^{2+}-cycling proteins in the three ventricular cell types (24, 37,39). These transmural differences in Ca^{2+}-cycling protein expression may explain the greater sensitivity of ENDO and MID cells to alternans (24). We previously reported that Ca^{2+} transients and contractions are longer in ENDO and MID than in EPI regions of the dog myocardium and that these differences are only in part the result of differences in APD, since contractions and Ca^{2+} transients are longer in ENDO than in EPI and MID cells when elicited with square pulses of fixed duration under voltage-clamp conditions (6). Under current-clamp conditions, the longer APD of the MID cells yields EC coupling kinetics that display slower relaxation in MID cells, similar to that of ENDO cells. Our results are consistent with those of Wan et al. (36), suggesting that a slower decay of the ENDO Ca^{2+} transients underlies their greater susceptibility to develop alternans.

The longer duration of the Ca^{2+} transient in ENDO (6,24) may be due a lower level of sarcoendoplasmic reticulum (SERCA) 2a and phospholamban in ENDO vs. EPI (24). MID cells have an intermediate expression of SERCA2a proteins (24) but display transients more similar to EPI than to ENDO cells when evoked by square pulses of constant duration. Thus MID cells show shorter transients and contractions under voltage-clamp conditions but much slower relaxation when activated with the long AP characteristic of this cell type. It is therefore not surprising that Ca^{2+} alternans develops preferentially in ENDO and MID ventricular cell layers. As the diastolic interval is abbreviated, there is progressively less time for reuptake and translocation of Ca^{2+} from cytoplasm to the junctional SR for rerelease. At fast rates, the process is incomplete in cells with a long Ca^{2+} transient, particularly following a large release. Consequently, a large release is followed by a small release, and visa versa. The alternation in Ca^{2+} cycling leads to beat-to-beat variation in inward and outward currents, principally Na^{+}-Ca^{2+} exchange current (I_{NaCa}), I_{Ca}, and slow delayed rectifier K^{+} current (I_{Ks}), leading to alternation in APD and T wave amplitude.

Region-specific development of subcellular alternans

Two recent studies have reported oscillations in Ca^{2+} release in different intracellular regions within individual myocytes (subcellular alternans). Subcellular alternans could be induced by rapid pacing in atrial but not in ventricular myocytes (22). It was also possible to induce “subcellular” alternans in atrial myocytes in the presence of glycolytic inhibition induced by pyruvate, iodoacetic acid, 2-deoxyglucose, and the fatty acid β-hydroxybutyrate (22). Our results are the first to demonstrate that this behavior also occurs in normal dog ventricular myocytes under conditions of rapid pacing. Although the mechanism for subcellular alternans is uncertain, our results tend to suggest that the development of subcellular alternans is related to SR function.

Dependence of Ca^{2+} alternans on SR

As a further assessment of the role of the SR function in the development of TWA, we examined the effects of pacing on Ca^{2+} transients in ventricular myocytes from 2-wk-old animals. Immunocytochemistry displayed RyRs reflecting sarcomeric organization but no organized t-tubules. Available evidence suggests that E-C coupling occurs as a result of direct myofilament activation by Ca^{2+} entering via L-type Ca^{2+} channels as well as via Na^{+}/Ca^{2+} exchange (14). The fact that Ca^{2+} alternans does not occur under these conditions supports the hypothesis that SR Ca^{2+} release and normal SR function are critical for the development of alternans.

Our data demonstrated that cells exhibiting a slower decay of the Ca^{2+} transient were more susceptible to the development of alternans during faster pacing conditions. We also demonstrated that, in cardiac cells lacking a well-organized SR (neonate ventricular cells), alternans were rarely observed. These data, coupled with the observation that alternans is abolished when SR function is impaired by treatment with ryanodine (33), provide further evidence in support of the hypothesis that SR Ca^{2+} cycling is a major component in the development of alternans.

Acknowledgements

We thank Bob Goodrow, Judy Hefferon, and Art Iodice for excellent technical assistance.

GRANTS

This study was supported by grants from the American Health Assistance Foundation (J. M. Cordeiro) and National Institutes of Health Grants HL-47678 (C. Antzelevitch) and AA-013915 (J. A. Wasserstrom).

References

1. Antzelevitch C, Sicouri S, Litovsky SH, Lukas A, Krishnan SC, Di Diego JM, Gintant GA, Liu DW. Heterogeneity within the ventricular wall. Electrophysiology and pharmacology of epicardial, endocardial, and M cells. Circ Res 1991;69:1427–1449. [PubMed: 1659499]
2. Blatter LA, Kockskamper J, Sheehan KA, Zima AV, Huser J, Lipsius SL. Local calcium gradients during excitation-contraction coupling and alternans in atrial myocytes. J Physiol 2003;546:19–31. [PubMed: 12509476]
3. Bouchard RA, Clark RB, Giles WR. Effects of action potential duration on excitation-contraction coupling in rat ventricular myocytes. Action potential voltage-clamp measurements. Circ Res 1995;76:790–801. [PubMed: 7728996]
4. Clark RB, Bouchard RA, Salinas-Stefanon E, Sanchez-Chapula J, Giles WR. Heterogeneity of action potential waveforms and potassium currents in rat ventricle. Cardiovasc Res 1993;27:1795–1799. [PubMed: 8275526]
5. Cordeiro JM, Bridge JH, Spitzer KW. Early and delayed afterdepolarizations in rabbit heart Purkinje cells viewed by confocal microscopy. Cell Calcium 2001;29:289–297. [PubMed: 11292386]
6. Cordeiro JM, Greene L, Heilmann C, Antzelevitch D, Antzelevitch C. Transmural heterogeneity of calcium activity and mechanical function in the canine left ventricle. Am J Physiol Heart Circ Physiol 2004;286:H1471–H1479. [PubMed: 14670817]
7. Cordeiro JM, Spitzer KW, Giles WR, Ershler PE, Cannell MB, Bridge JH. Location of the initiation site of calcium transients and sparks in rabbit heart Purkinje cells. J Physiol 2001;531:301–314. [PubMed: 11310434]
8. Diaz ME, O'Neill SC, Eisner DA. Sarcoplasmic reticulum calcium content fluctuation is the key to cardiac alternans. Circ Res 2004;94:650–656. [PubMed: 14752033]
9. Di Diego JM, Belardinelli L, Antzelevitch C. Cisapride-induced transmural dispersion of repolarization and torsade de pointes in the canine left ventricular wedge preparation during epicardial stimulation. Circulation 2003;108:1027–1033. [PubMed: 12912819]

10. Di Diego JM, Cordeiro JM, Goodrow RJ, Fish JM, Zygmunt AC, Perez GJ, Scornik FS, Antzelevitch C. Ionic and cellular basis for the predominance of the Brugada syndrome phenotype in males. Circulation 2002;106:2004–2011. [PubMed: 12370227]
11. Fedida D, Giles WR. Regional variations in action potentials and transient outward current in myocytes isolated from rabbit left ventricle. J Physiol 1991;442:191–209. [PubMed: 1665856]
12. Fox JJ, McHarg JL, Gilmour RF Jr. Ionic mechanism of electrical alternans. Am J Physiol Heart Circ Physiol 2002;282:H516–H530. [PubMed: 11788399]
13. Haddock PS, Coetzee WA, Cho E, Porter L, Katoh H, Bers DM, Jafri MS, Artman M. Subcellular [Ca2+]i gradients during excitation-contraction coupling in newborn rabbit ventricular myocytes. Circ Res 1999;85:415–427. [PubMed: 10473671]
14. Harrison SM. The voltage dependence of contraction at different stimulation rates in guinea-pig ventricular myocytes. Exp Physiol 1995;80:941–958. [PubMed: 8962709]
15. Hua F, Johns DC, Gilmour RF Jr. Suppression of electrical alternans by overexpression of HERG in canine ventricular myocytes. Am J Physiol Heart Circ Physiol 2004;286:H2342–H2351. [PubMed: 14962839]
16. Hund TJ, Rudy Y. Rate dependence and regulation of action potential and calcium transient in a canine cardiac ventricular cell model. Circulation 2004;110:3168–3174. [PubMed: 15505083]
17. Huser J, Lipsius SL, Blatter LA. Calcium gradients during excitation-contraction coupling in cat atrial myocytes. J Physiol 1996;494:641–651. [PubMed: 8865063]
18. Jordan PN, Christini DJ. Action potential morphology influences intracellular calcium handling stability and the occurrence of alternans. Biophys J 2006;90:672–680. [PubMed: 16239324]
19. Jorgensen AO, Shen AC, Arnold W, McPherson PS, Campbell KP. The Ca2+-release channel/ryanodine receptor is localized in junctional and corbular sarcoplasmic reticulum in cardiac muscle. J Cell Biol 1993;120:969–980. [PubMed: 8381786]
20. Kaprielian R, Sah R, Nguyen T, Wickenden AD, Backx PH. Myocardial infarction in rat eliminates regional heterogeneity of AP profiles, I_{to} K^+ currents, and $[Ca^{2+}]_i$ transients. Am J Physiol Heart Circ Physiol 2002;283:H1157–H1168. [PubMed: 12181147]
21. Klingenheben T, Zabel M, D'Agostino RB, Cohen RJ, Hohnloser SH. Predictive value of T-wave alternans for arrhythmic events in patients with congestive heart failure. Lancet 2000;356:651–652. [PubMed: 10968440]
22. Kockskamper J, Blatter LA. Subcellular Ca2+ alternans represents a novel mechanism for the generation of arrhythmogenic Ca2+ waves in cat atrial myocytes. J Physiol 2002;545:65–79. [PubMed: 12433950]
23. Lakireddy V, Baweja P, Syed A, Bub G, Boutjdir M, El-Sherif N. Contrasting effects of ischemia on the kinetics of membrane voltage and intracellular calcium transient underlie electrical alternans. Am J Physiol Heart Circ Physiol 2005;288:H400–H407. [PubMed: 15345492]
24. Laurita KR, Katra R, Wible B, Wan X, Koo MH. Transmural heterogeneity of calcium handling in canine. Circ Res 2003;92:668–675. [PubMed: 12600876]
25. Litovsky SH, Antzelevitch C. Transient outward current prominent in canine ventricular epicardium but not endocardium. Circ Res 1988;62:116–126. [PubMed: 2826039]
26. Litwin SE, Li J, Bridge JH. Na-Ca exchange and the trigger for sarcoplasmic reticulum Ca release: studies in adult rabbit ventricular myocytes. Biophys J 1998;75:359–371. [PubMed: 9649393]
27. Liu DW, Gintant GA, Antzelevitch C. Ionic bases for electrophysiological distinctions among epicardial, midmyocardial, and endocardial myocytes from the free wall of the canine left ventricle. Circ Res 1993;72:671–687. [PubMed: 8431990]
28. Malone JE, Cordeiro JM, Aistrup GL, Cianfrocco M, Scornik FS, Antzelevitch C, Wasserstrom JA. Identification of cellular and subcellular alternans by confocal microscopy in the canine left ventricle (Abstract). Biophys J 2006;90:2702.
29. Picht E, DeSantiago J, Blatter LA, Bers DM. Cardiac alternans do not rely on diastolic sarcoplasmic reticulum calcium content fluctuations. Circ Res 2006;99:740–748. [PubMed: 16946134]
30. Sah R, Ramirez RJ, Backx PH. Modulation of Ca(2+) release in cardiac myocytes by changes in repolarization rate: role of phase-1 action potential repolarization in excitation-contraction coupling. Circ Res 2002;90:165–173. [PubMed: 11834709]

31. Sah R, Ramirez RJ, Oudit GY, Gidrewicz D, Trivieri MG, Zobel C, Backx PH. Regulation of cardiac excitation-contraction coupling by action potential repolarization: role of the transient outward potassium current [I(to)]. J Physiol 2003;546:5–18. [PubMed: 12509475]
32. Sedarat F, Xu L, Moore ED, Tibbits GF. Colocalization of dihydropyridine and ryanodine receptors in neonate rabbit heart using confocal microscopy. Am J Physiol Heart Circ Physiol 2000;279:H202–H209. [PubMed: 10899057]
33. Shimizu W, Antzelevitch C. Cellular and ionic basis for T-wave alternans under Long QT conditions. Circulation 1999;99:1499–1507. [PubMed: 10086976]
34. Sipido KR. Understanding cardiac alternans: the answer lies in the Ca2+ store. Circ Res 2004;94:570–572. [PubMed: 15031268]
35. Tibbits GF, Xu L, Sedarat F. Ontogeny of excitation-contraction coupling in the mammalian heart. Comp Biochem Physiol A Mol Integr Physiol 2002;132:691–698. [PubMed: 12095856]
36. Wan X, Laurita KR, Pruvot EJ, Rosenbaum DS. Molecular correlates of repolarization alternans in cardiac myocytes. J Mol Cell Cardiol 2005;39:419–428. [PubMed: 16026799]
37. Xiong W, Tian Y, DiSilvestre D, Tomaselli GF. Transmural heterogeneity of Na+-Ca2+ exchange: evidence for differential expression in normal and failing hearts. Circ Res 2005;97:207–209. [PubMed: 16002750]
38. Yang ZK, Boyett MR, Janvier NC, Hulme JT, Orchard CH, Colyer J. Differences in the time course of contraction in subepicardial and subendocardial cells isolated from the left ventricle of dog and ferret (Abstract). J Physiol 1995;487:127P.
39. Zygmunt AC, Goodrow RJ, Antzelevitch C. $I_{Na\text{-}Ca}$ contributes to electrical heterogeneity within the canine ventricle. Am J Physiol Heart Circ Physiol 2000;278:H1671–H1678. [PubMed: 10775148]

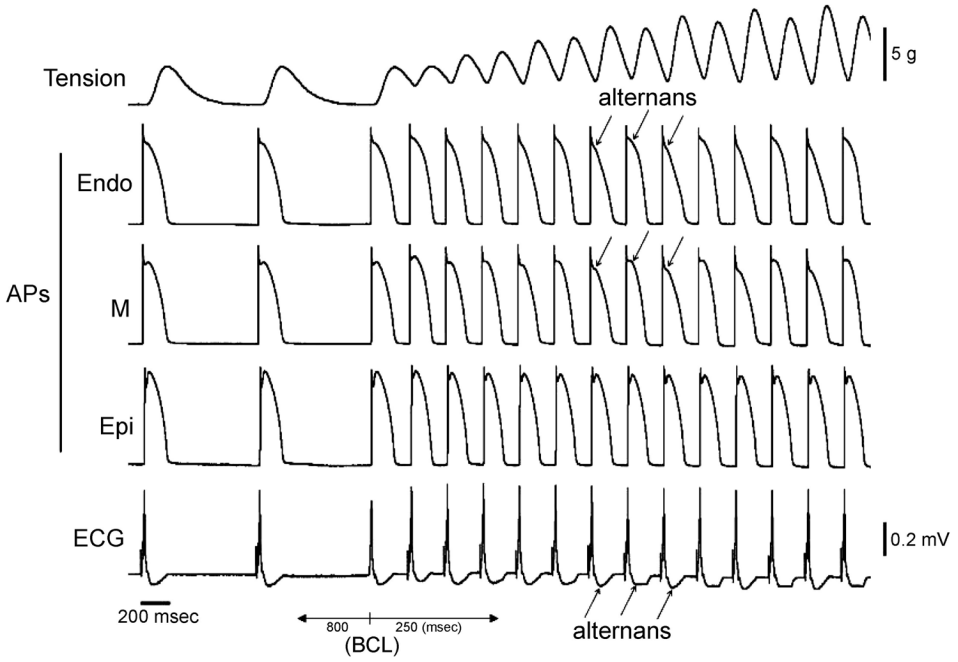

Fig. 1.

Ventricular wedges were paced at a cycle length of 800 ms using bipolar electrodes in contact with the endocardial surface. After the cycle length was reduced to 250 ms for 15–30 s, the development of electrical alternans is apparent in epicardial (EPI) and midmyocardial (MID) action potentials. The tension recording exhibits mechanical alternans, and ST-T wave alternans can be seen in the electrocardiographic (ECG) trace.

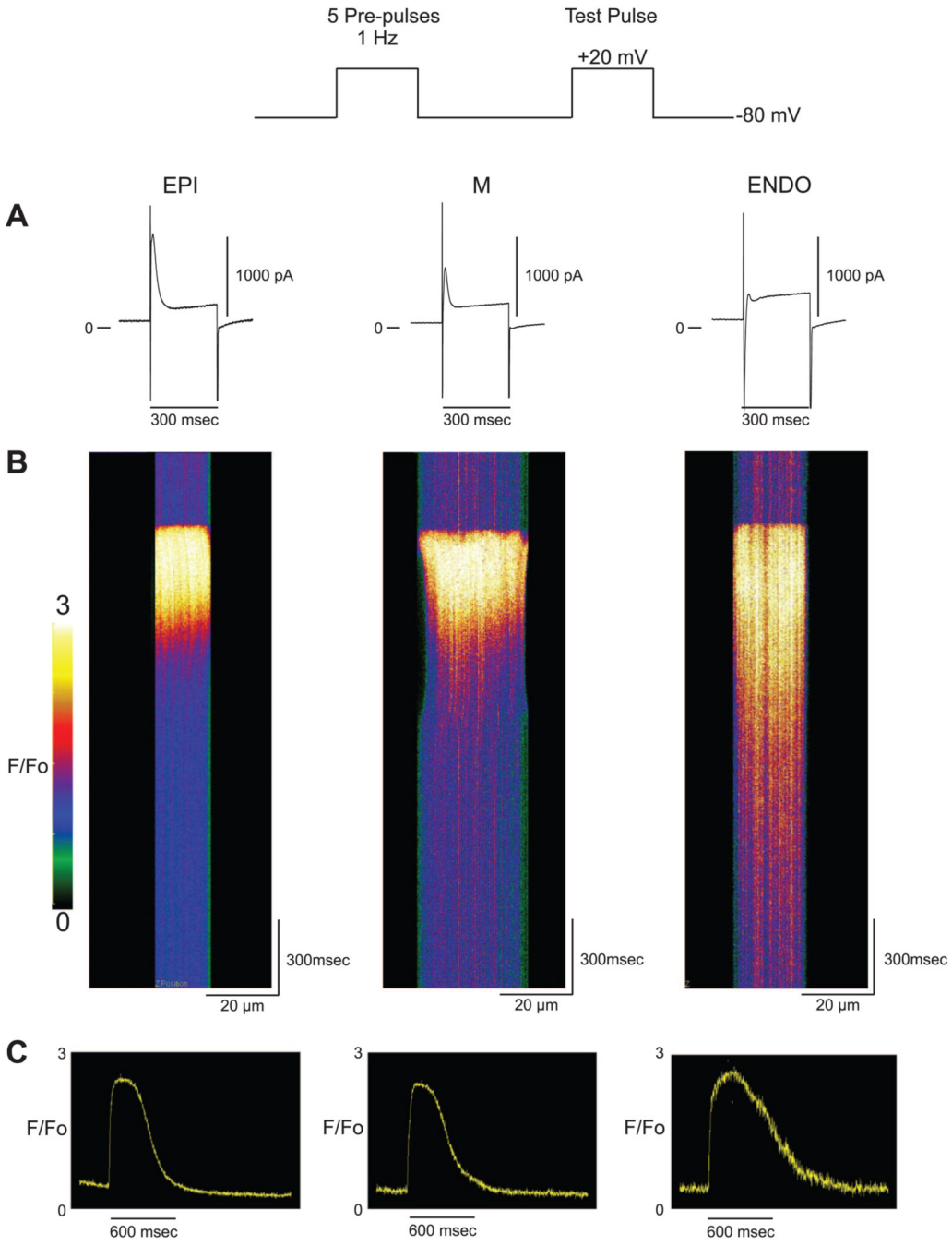

Fig. 2.

Representative recording of ionic currents (*A*) and corresponding confocal xt line scans (*B*) from an EPI, endocardial (END), and MID cell recorded under voltage clamp. The voltage-clamp protocol is shown at *top*. Five prepulses were applied to the myocytes to maintain a constant sarcoplasmic reticulum (SR) load. Following application of a 300-ms test pulse to +20 mV, a large transient outward current (I_{to}) can be observed in the EPI and MID cell (*A*). The corresponding line scan recordings (*B*) and time course of F/F_0 (*C*) for EPI and MID cells show similar kinetics. In contrast, the line scan recorded from the END cell has a much slower decay compared with the other two cell types.

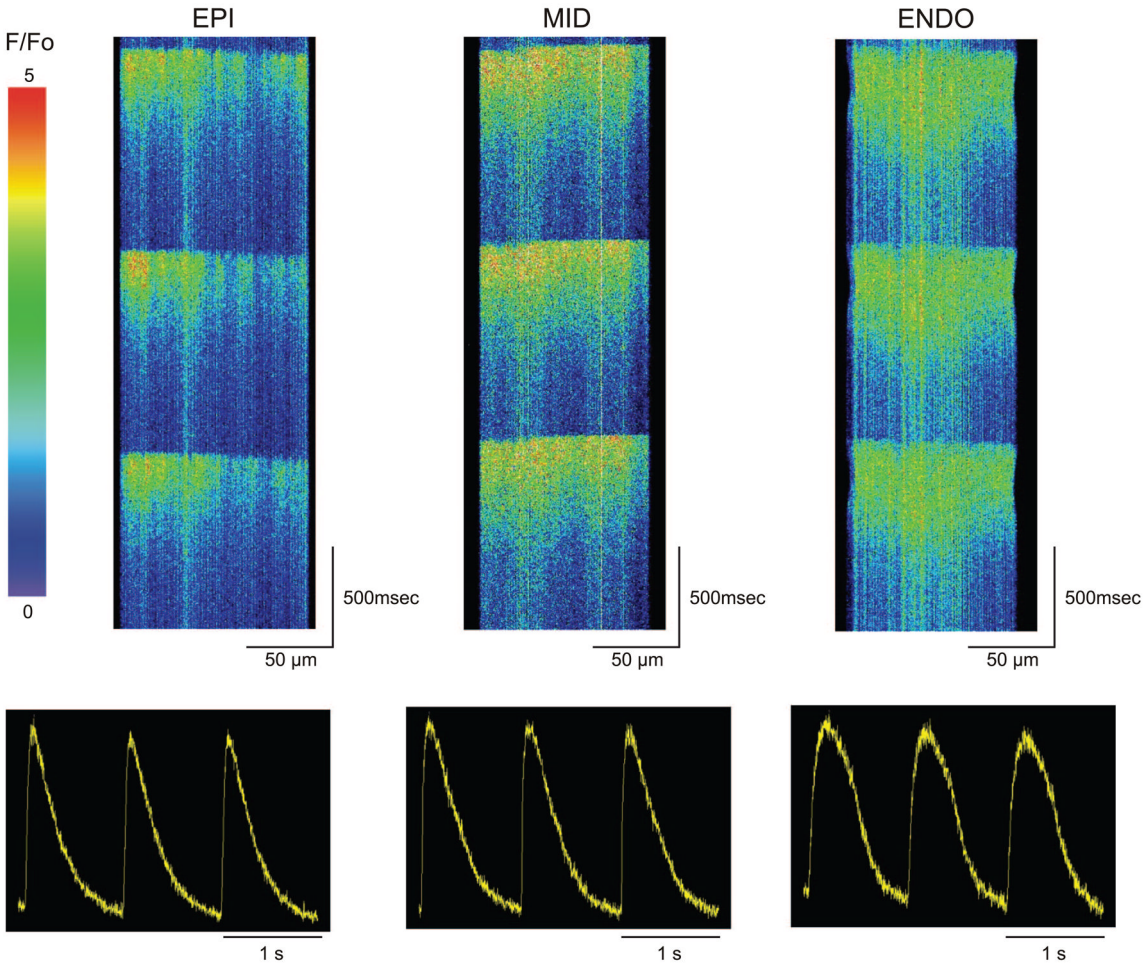

Fig. 3.

Representative line scans recorded from an EPI, MID, and ENDO ventricular myocyte (*top*). The myocytes were field stimulated at a cycle length of 1,000 ms. Myocytes from the 3 cell layers exhibited a rapid and uniform rise in fluorescence. However, the decay of fluorescence was slowest in ENDO cells. *Bottom*: time course of F/F_o in the 3 cell types.

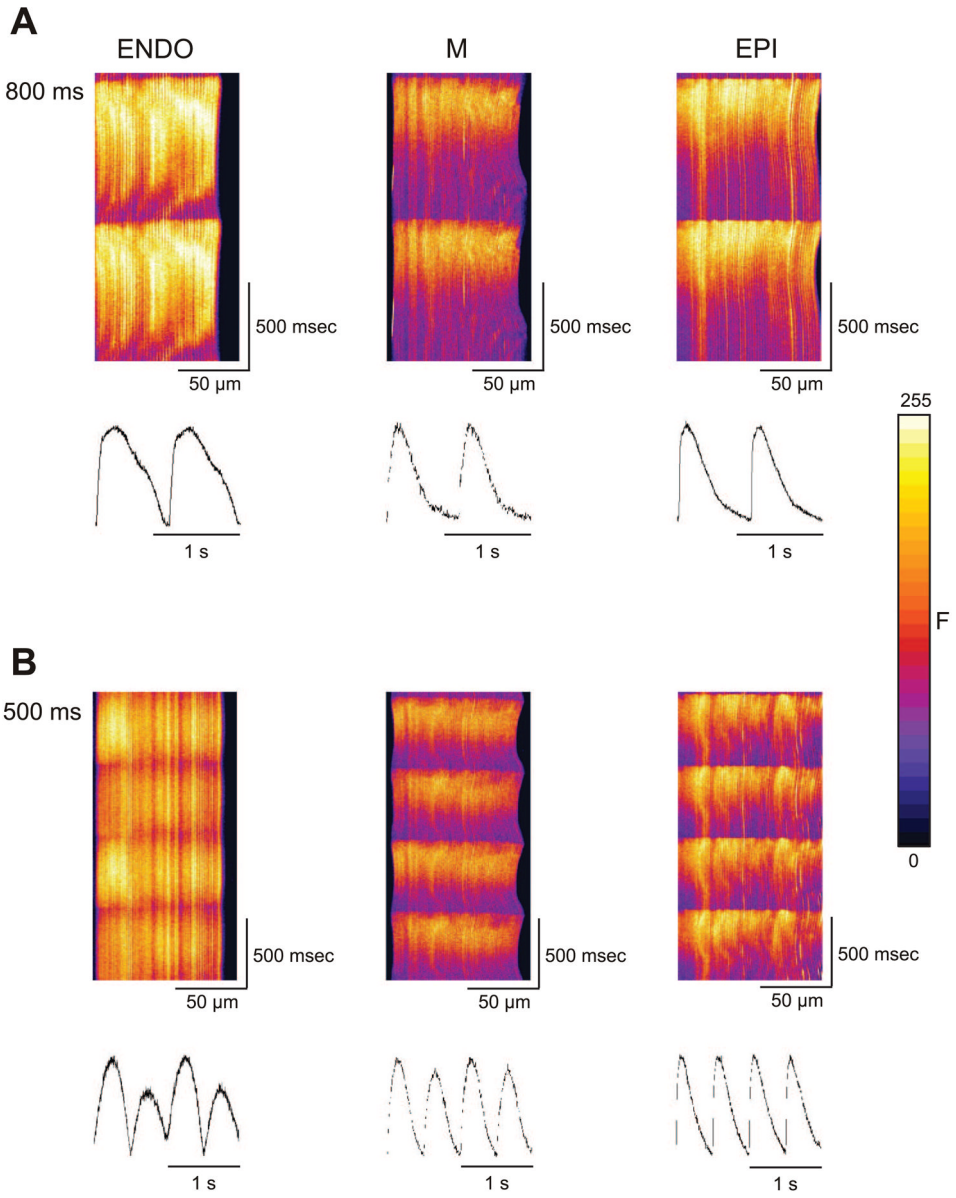

Fig. 4.

Representative line scans and time course of F/F_o recorded from the 3 ventricular cell types. *A*: scans at a cycle length of 800 ms. To induce alternans, cells were paced at progressively faster cycle lengths. *B*: line scans recorded at a cycle length of 500 ms show the appearance of alternans in the ENDO and MID region.

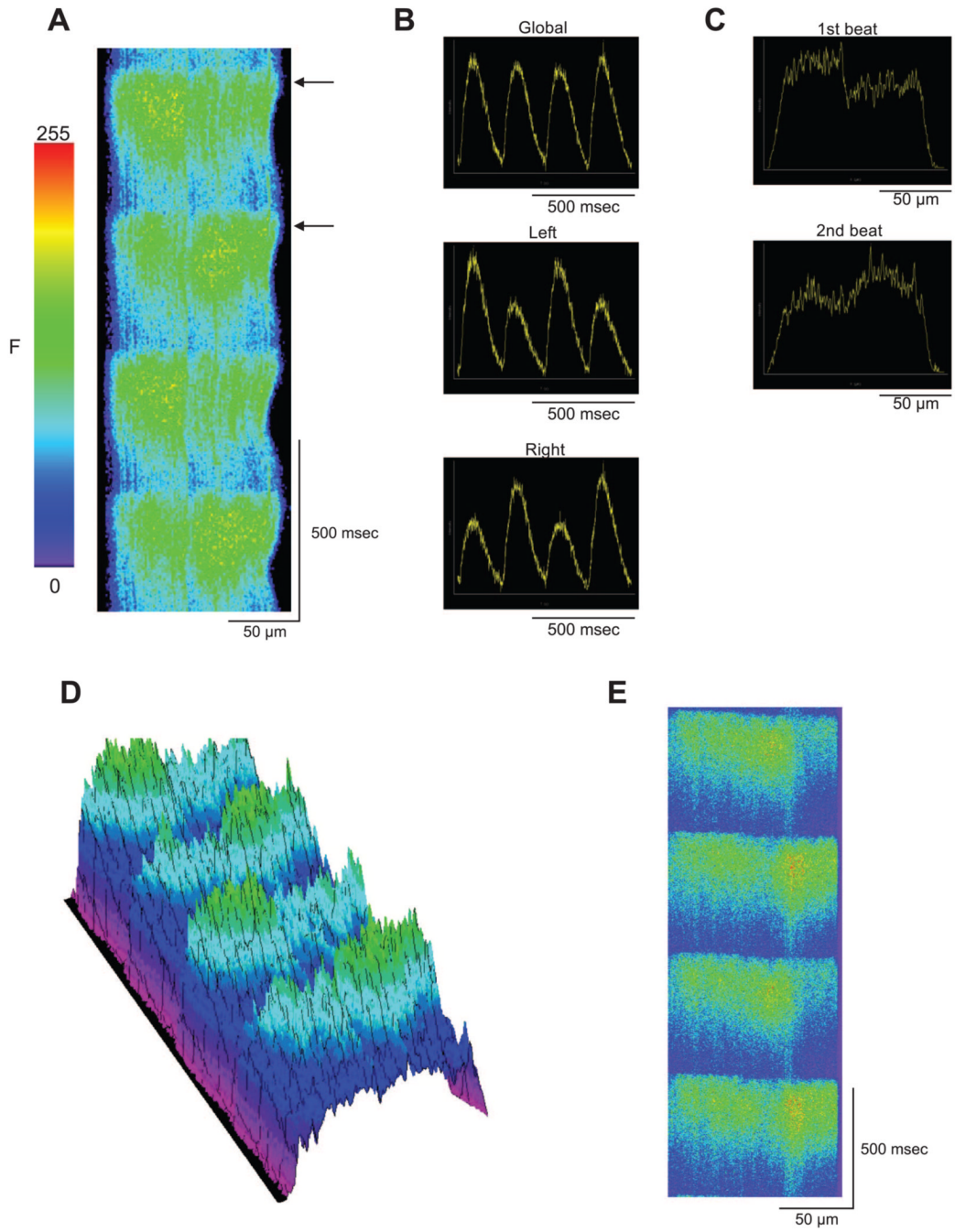

Fig. 5.

A: representative line scan image showing subcellular alternans. *B*: the integrated global fluorescence trace appears uniform and does not show any alternation. However, when one only half of the cell is analyzed, alternans is plainly apparent. *C*: analysis of the space plot from 2 successive beats shows heterogeneity of the Ca^{2+} levels across the length of the cell (black arrows in *A*). *D*: 3-dimensional reconstruction of *A*. This provides an impression of the distribution of Ca^{2+} during subcellular alternans. The alternans occurring in half the cell is clearly out of phase with alternans in the other half of the cell. *E*: representative line scan image showing that subcellular alternans occurs in the presence of latrunculin B and cytochalasin D.

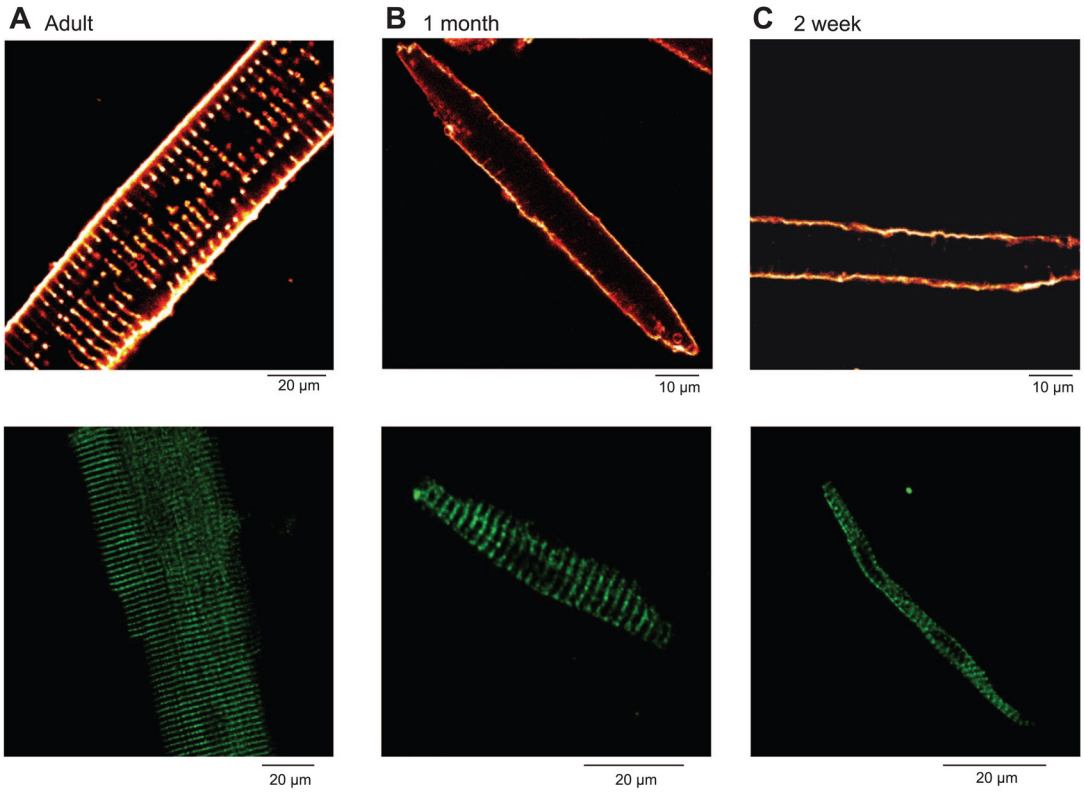

Fig. 6.

Ventricular cells isolated from dogs at various stages of development stained with the membrane dye di-8-ANEPPS (*A–C*, *top*). The t-tubular structure can be seen in adult cells (*A*, *top*). In contrast, ventricular cells from 2-wk-old dogs show no t-tubules (*C*, *top*), whereas 4-wk-old ventricular cells show t-tubules in a formative stage of development (*B*, *top*). Immunohistochemical localization of ryanodine receptors (RyR2) in ventricular cells (*A–C*, *bottom*) are shown. The adult ventricular cell shows prominent bands of RyR2 staining at the level of the t-tubules, suggesting a well-developed SR (*A*, *bottom*). The RyR2 organization in ventricular cells from 2-wk-old dogs (*C*, *bottom*) does not appear as well organized.

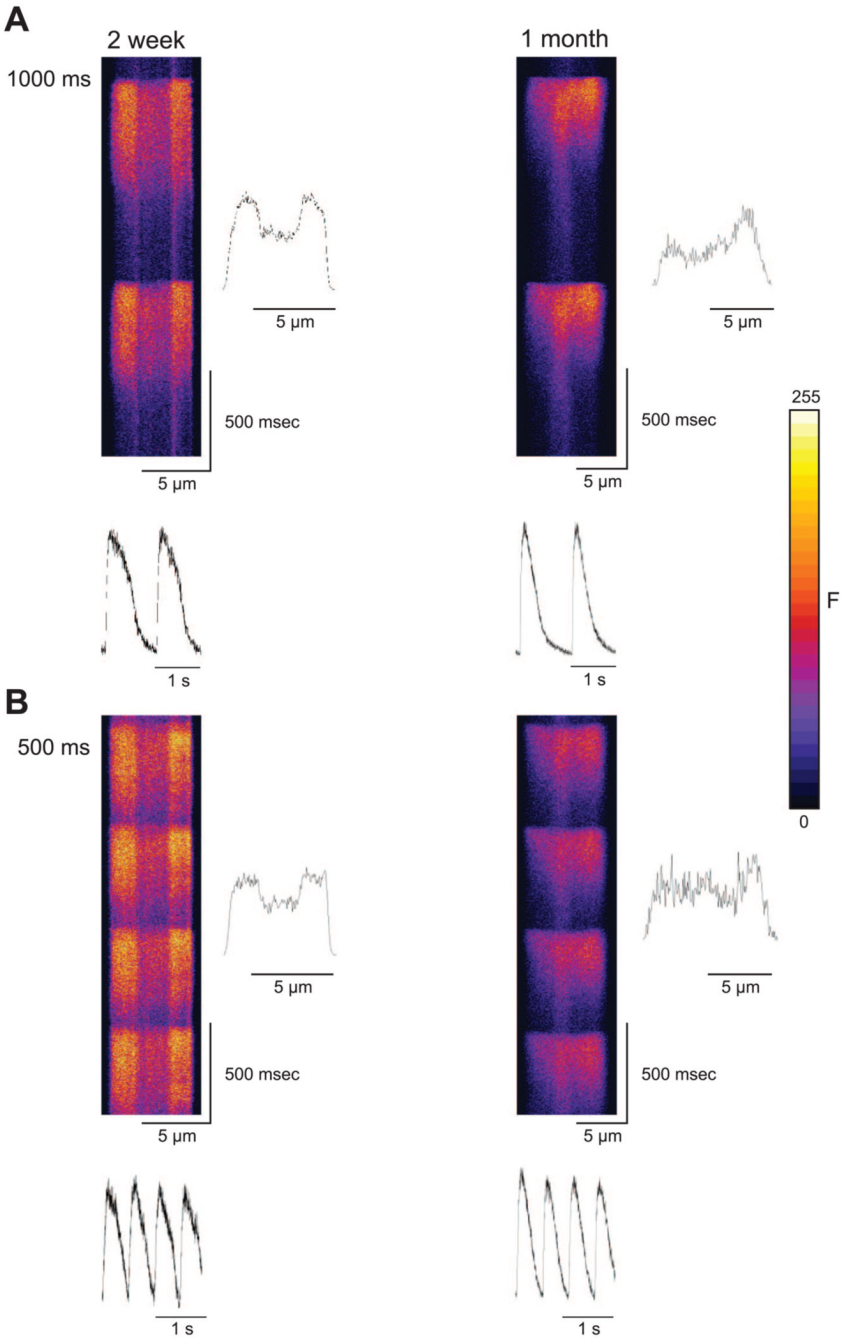

Fig. 7.

Representative line scans recorded from a 2-wk and 1-mo ventricular myocyte at a cycle length of 1,000 ms (*A*) and 500 ms (*B*). Under rapid pacing conditions, alternans could not be induced in ventricular cells from 2-wk-old dogs but could occasionally be seen in ventricular cells from 1-mo-old animals.